Int. J. Electrochem. Sci., 9 **(2014)** 4840 - 4853

International Journal of
ELECTROCHEMICAL
SCIENCE
www.electrochemsci.org

Poly(3-methoxythiophene/ 3,4-ethylenedioxythiophene) Films Electrodeposited in Two Hydrophilic/ Hydrophobic Imidazolium Ionic Liquids: Voltammetric, UV/Vis Spectroelectrochemical, and AFM Morphology Comparisons

Abebaw A. Tsegaye[1], *Tesfaye T. Waryo*[1,*], *Shimelis Admassie*[2], *Emmanuel I. Iwuoha*[1]

[1]Department of Chemistry, University of the Western Cape, 7535 Bellville, South Africa
[2]Departments of Chemistry, Addis Ababa University, P.O.Box 1176, Addis Ababa, Ethiopia
[*]E-mail: twaryo@uwc.ac.za

Received: 9 April 2014 / *Accepted:* 21 May 2014 / *Published:* 16 June 2014

Electropolymerization and electro-co-polymerization of 3-methoxythiophene (MOT) and 3, 4-ethylenedioxythiophene (EDOT) in the ionic liquids (ILs) 1-butyl-3-methylimidazolium terafluoroborate ($BMIm^+BF_4^-$) and 1-octyl-3-methylimidazolium bis(trifluoromethylsulfonyl)imide ($OMIm^+Tf_2N^-$) as well as the voltammetric, UV/Vis absorption spectroelectrochemical and micromorphological properties of the resulting polymer films are compared and contrasted. MOT was oxidized at a lower potential than EDOT in the hydrophilic $BMIm^+BF_4^-$, but the reverse being true in the hydrophobic $OMIm^+Tf_2N^-$. The MOT/EDOT mixture's oxidation-onset potentials were similar in the two ILs. Post-electropolymerization cyclic voltammograms (CVs) showed the deposition of electroactive thin films which didn't dissolve-off. Among the other observations are that UV/Vis absorption spectra indicated $OMIm^+Tf_2N^-$ resulted in polymer molecules with higher degree of conjugation and more heterogeneous polymer films than did $BMImBF_4$, and according to AFM images thicker and rougher films were obtained in the latter IL.

Keywords: methoxythiophene; ethylenedioxythiophene; imidazolium ionic liquids; electropolymerization; polythiophenes; conducting polymer

1. INTRODUCTION

The advent of room temperature ionic liquid compounds (ILs) has made available to the electrochemist a new class of electrolytes which themselves act as practically non-volatile solvents with excellent intrinsic electrical conductivity and electrochemical stability over a much wider range of electrode potentials in contrast with traditional organic electrolyte solutions [1-4]. In the application area of electro-synthesis, the solvent-electrolyte dual function of ILs brings about experimental simplification in preparation, handling, and recovery of the reaction medium. Of particular interest is their use for the electropolymerization of conducting polymers, where a number of ILs have been exploited to prepare polymers with improved electrochemical stability, and, in some cases, smoother and denser films than the ones obtained using traditional organic electrolytes[4-7]. Among the polymers whose successful electrochemical synthesis in ILs have reported are polypyrrole [8], poly(3-(4-fluorophenyl)thiophene [9], poly(3,4-ethylenedioxythiophene) [9-12], poly(para)phenylene [13], poly(3-chlorothiophene) [14], polythiophene [15] and nanopoly(3-methoxythiophene) [16].

The nature of the ions of the IL has been shown to strongly control the dynamics of electrochemically induced doping of a conducting polymer; hence, affecting the latter's electrochemical, morphological and other properties [4, 6]. For instance, the electropolymerization of pyrrole was found to be more efficient in 1-ethyl-3-methylimidazolium trifluoromethanesulfonate ($EMIm^+Tf^-$) (conductivity (σ) = 1.36 S m^{-1}, viscosity (η) = 42.7 cP at 25 ^OC) than in 1-ethyl-3-methylimidazolium hexafluorophosphate ($EMIm^+PF_6^-$) (σ = 0.52 S m^{-1}, η = 15.0 cP at 25 ^OC) and 1-ethyl-3-methylimidazolium tetrafloroborate ($EMIm^+BF_4^-$) (σ = 0.92 S m^{-1}, η = 31.8 cP at 25 ^OC) [8] indicated the influence the anion on the rate of polymerization of polyprrole as a result of change in the viscosity of ILs. *Ibid* observed among the polypyrrole (PPy) films obtained in the above three ILs the PPy formed in $EMIm^+Tf^-$ had microscopically smooth morphology and the highest degree of electrochemical p-doping. It has been suggested, taking into account the similar conductivities of these ILs, that the higher viscosity of $EMIm^+Tf^-$, caused by the presence of the anion Tf^- (or $CF_3SO_3^-$), might have favourably sustained electropolymerization process by reducing the diffusion of intermediates away from the vicinity of the electrode surface. Furthermore, this PPy film exhibited higher anodic/ cathodic peak current-densities when compared with a PPy film prepared in acetonitrile/ IL or water/IL solutions [8]. A study about the effect of variation of cations showed that electropolymerization of 3,4-ethylenedioxythiophene (EDOT) in N,N-butylmethylpyrrolidinium bis(trifloromethane-sulfonyl)imide ($BMPyr^+Tf_2N^-$) (η = 85 cP, σ = 2.2 mS cm^{-1} at 25^oC) proceeded more slowly than in the less viscous but much more conductive N – ethyl-N-methylimidazolium bis(trifluromethanesulfonyl)imide ($EMIm^+Tf_2N^-$) (η = 34 cP, σ = 8.8 mS cm^{-1} at 20^oC) [6]. In this case, the favourable effects of the higher viscosity of $BMPyr^+Tf_2N^-$ might have been outweighed by the advantage of the much higher conductivity of $EMIm^+Tf_2N^-$. The transport of reactants and ions to the electrode surface is decreased significantly in the pyrrolidinium ion-based IL. This showed the effects cations have on the physical properties of ILs and the electrochemical polymerization of EDOT. Thus, both the anion and cation components of an IL significantly influence the rate of electrochemical polymerization and properties of the polymer produced.

This report presents the electropolymerization and electro-co-polymerization of 3-methoxythiophene (MOT) and 3, 4-ethylenedioxythiophene (EDOT) in 1-butyl-3-methylimidazolium terafluroborate ($BMIm^+BF_4^-$), a hydrophilic IL, and 1-octyl-3-methylimidazolium bis(trifluoromethylsulfonyl)imide ($OMIm^+Tf_2N^-$), a hydrophobic IL, as well as the voltammetric, UV/Vis spectroelectrochemical, and atomic force microscopic comparisons of the resulting films. $BMIm^+BF_4^-$ has a higher viscosity and conductivity (η = 154 cP, σ = 0.28 S m^{-1} at 293.1 K) [4, 17] than $OMIm^+Tf_2N^-$ (η = 96 cP, σ = 0.75 S m^{-2} at 293.1K) [18].

2. EXPERIMENTAL

2.1. Chemicals

3-methoxythiophene (MOT) (98%), 3, 4-ethylenedioxythiophene (EDOT) (99%), lithium perchlorate (95%), acetonitrile anhydrous (99.8%), ferrocene (98%), were purchased from Aldrich and used as received. Alumina polishing powders (1, 0.3, and 0.05 μm) were purchased from Buehler (Germany). 1-buthyl-3-methylimidazolium tetrafluroborate ($BMIm^+BF_4^-$) (Aldrich) and 1-octyl-3-methylimidazolium bis(trifluoromethylsulfonyl)imide ($OMIm^+Tf_2N^-$) (Merck) were used without further purification. Millipore water (resistivity = 18 MΩ cm) was used to prepare aqueous solutions.

2.2. Instrumentation

Electrochemical experiments were performed using BAS100B and BASi Epsilon electrochemical analyzers and a three – electrode cell a glassy carbon disc working electrode (GCE, ∅ = 3.0 mm), a Pt wire auxiliary electrode, and a second Pt wire pseudo reference electrode. Spectroelectrochemical experiments were performed using a specially designed quartz cuvette cell (1 mm × 10 × mm, Bioanalytical Systems, Inc) and the Nicolet E100 UV/vis absorption spectrometer (Thermo-Electron Corporation). In this case the working electrode was an ITO coated glass and the auxiliary electrode was a platinum-gauze. The ITO/glass (7 mm × 50 mm × 0.6 mm, $R \leq 10\ \Omega$) was supplied by Delta Technologies Inc (Loveland, USA) and used as received after rinsing with deionized water. Atomic force microscopy (AFM) imaging of polymer films electrodeposited on the ITO electrodes were done using a Veeco NanoMan V model AFM microscope with a silicon tip of spring constant 1-5 N/m and resonance frequency 60 – 100 kHz.

2.3. Electrochemical Polymerization and Characterization

Cyclic voltammetric electropolymerization of 3-methoxythiophene (MOT), 3,4-ethylenedioxythiophene (EDOT), and a 1:1 MOT/EDOT mixture were carried at same concentrations of 0.1 M dissolved in $BMIm^+BF_4^-$ and $OMIm^+Tf_2N^-$ using the three electrode cell described in section 2.2 Before use, the GCE's surface was cleaned to a shiny finish by consecutively polishing with 1 μm, 0.3 μm and 0.05 μm alumina polishing powders, rinsing with deionized water after each polishing steps, and followed by ultrasonic cleaning in deionized water and ethanol consecutively and finally rinsing with acetone. Before an electrochemical experiment was started, the electrolyte medium was always purged with Ar gas and overflow of the gas was maintained during the run. The resulting polymer films, PMOT from MOT, PEDOT from EDOT, and PMEDOT from MOT/EDOT mixture, were rinsed with deionized water and transferred to fresh IL or aq. $LiClO_4$ (0.1 M) for characterization by cyclic voltammetry. Potentials in the results reported are relative to the redox potential of the ferrocene/ferrocenium (Fc/Fc^+) system (1 mM). All experiments were performed at room temperature (20 ^oC).

2.4. UV-Vis Spectroelectrochemistry

The ITO/glass transparent electrodes were now used instead of the GCE to carry out the electropolymerization described in section 2.3. The resulting polymer film-coated ITO electrodes were then rinsed with deionized water, transferred to the UV/Vis spectro-electrochemical cell filled with aqueous $LiClO_4$ (0.1 M) to record absorption spectra of neutral and oxidized films.

3. RESULTS AND DISCUSSIONS

3.1. Electropolymerization/ Electro-co-polymerization

The cyclic voltammograms (CVs) of the electropolymerization of MOT, EDOT, and a 50% MOT/EDOT mixture dissolved in $BMIm^+BF_4^-$ or $OMIm^+Tf_2N^-$ are shown in Figure 1 (a) to (f). The resulting polymer films: PMOT, PEDOT, and PMEDOT are respectively referred to as PMOT1, PEDOT1, and PMEDOT1 if electrodeposited in $BMIm^+BF_4^-$, and as PMOT2, PEDOT2, and PMEDOT2 in $OMIm^+Tf_2N^-$.

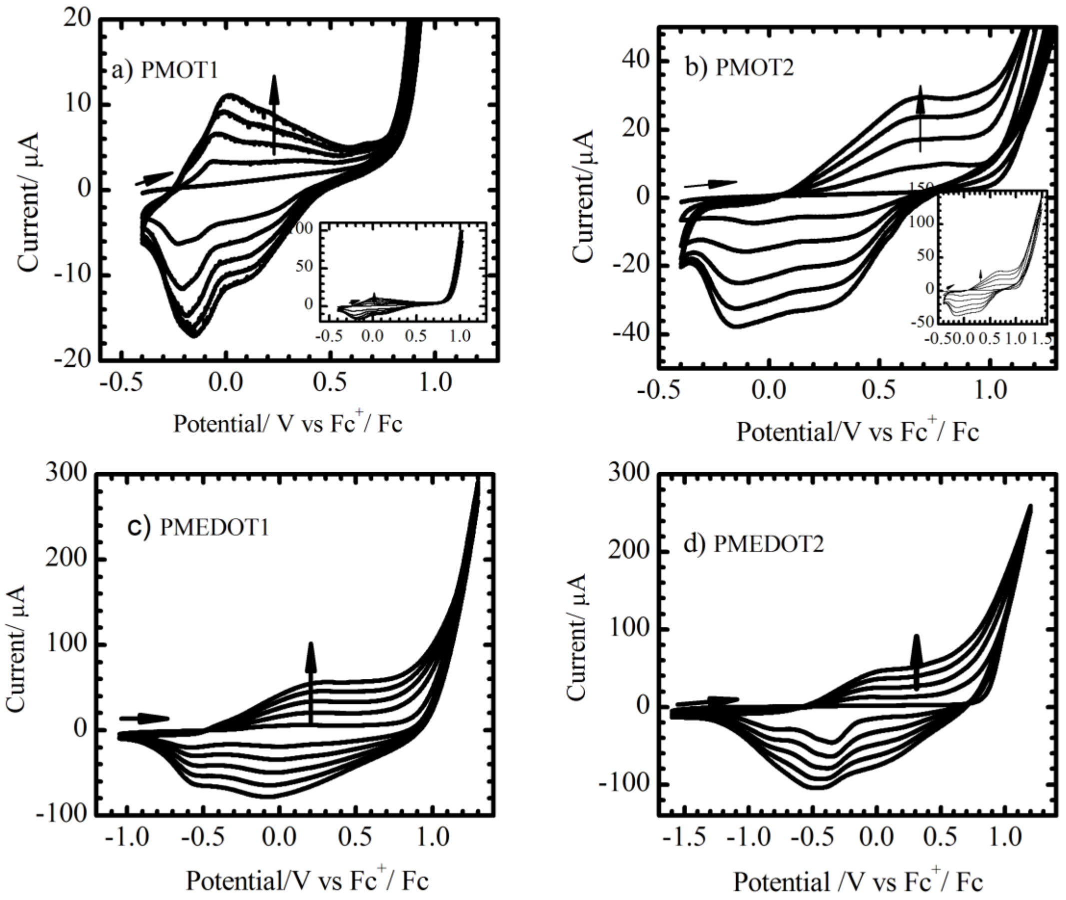

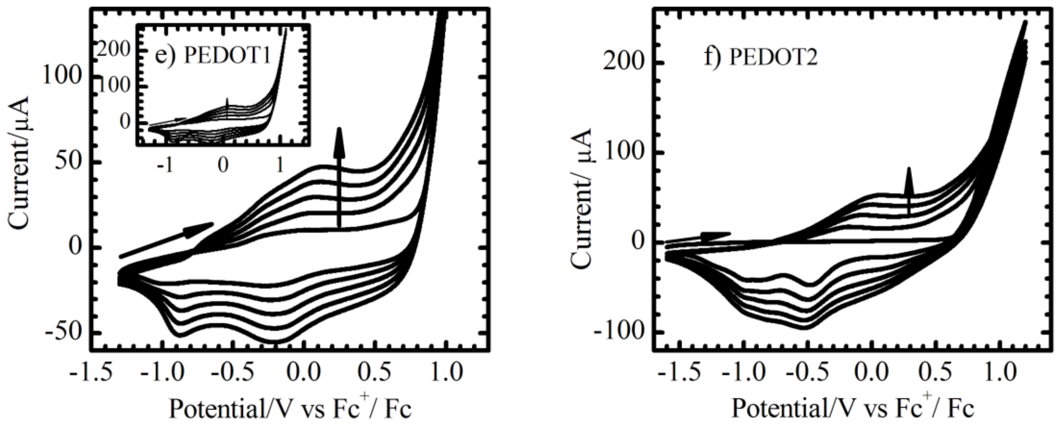

Figure 1. Electropolymerization of MOT (a, b), EDOT (e, f), & MOT/EDOT (1:1) (c, d), 0.1 M each, at a GC electrode in $BMIm^+BF_4^-$ (a, c, e) & $OMIm^+Tf_2N^-$ (b, d, f). Scan rate = 50 mV/s.

As can be read from the corresponding first anodic scan voltammograms, the onset potentials ($E_{ox\text{-}onset}$) of the oxidation of MOT in both ILs were about 1.04 V vs Fc^+/Fc (or 1.35 vs SCE) and higher than literature values (1.39, 1.2, 1.1 and 1.08 V vs. SCE) [19-22]. That of EDOT was about 0.75 V in $OMIm^+Tf_2N^-$ and 1.12 V in $BMIm^+BF_4^-$. Thus, in $BMIm^+BF_4^-$, MOT was oxidized at a lower potential than EDOT, but the reverse being true in $OMIm^+Tf_2N^-$. The MOT/EDOT mixture's $E_{ox\text{-}onset}$ in the two ILs were also similar (1.10 V in $OMIm^+Tf_2N^-$ & 1.14 V in $BMIm^+BF_4^-$), but its post-onset current-potential (i/E) curve resembled that of the more easily oxidizable component (lower $E_{ox\text{-}onset}$) in a given IL. However, the overall magnitude of current and shape of the mixture's electropolymerization CV was always dominated by EDOT/ PEDOT electrochemistry.

The net-charge (Q_{net}) consumed during each monomer's or mixture's electropolymerization in $OMIm^+Tf_2N$ was twice as high as that in $BMIm^+BF_4^-$, implying that in the former IL a higher yield of polymer film could be expected.

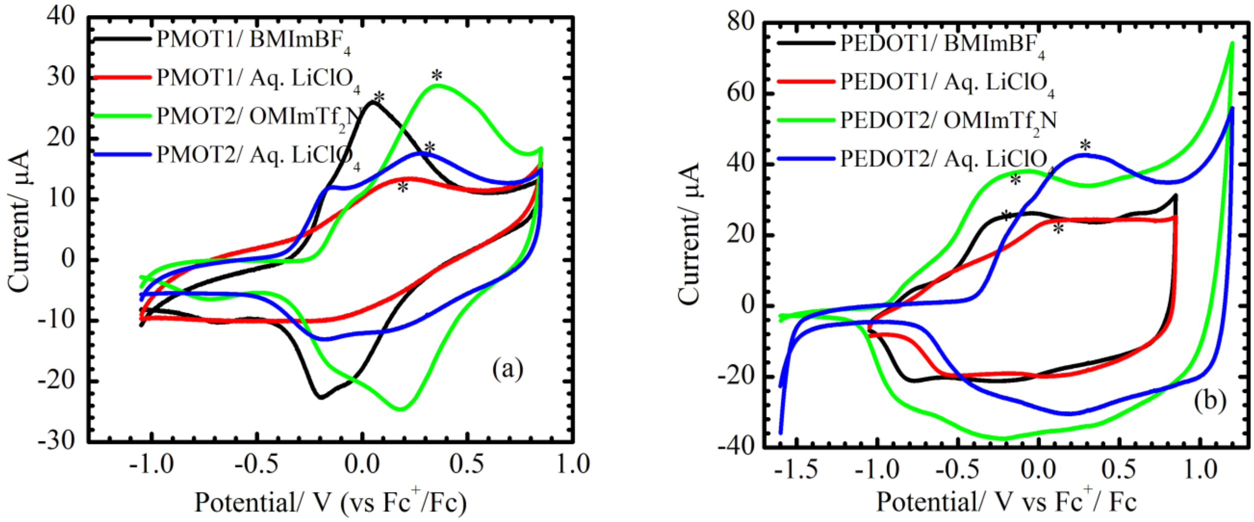

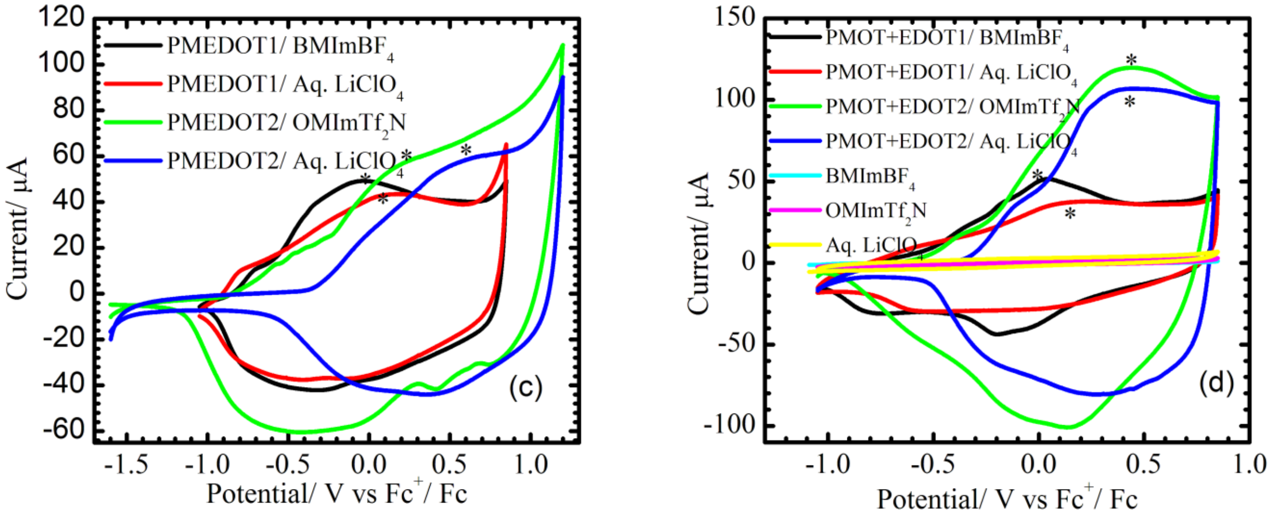

Figure 2. CVs of the films in fresh portions the two ILs & aq. $LiClO_4$. (a) PMOT1 & PMOT2; (b) PEDOT1 & PEDOT2; and, (c) PMEDOT1 & PMEDOT2. (d) CVs predicted for PMEDOT by summing CVs in (a) and (b). Scan rate = 50 mV s^{-1}. Initial scan = anodic.

Possibly the lower viscosity of $OMIm^+Tf_2N^-$ allowed a faster diffusion of monomer molecules towards the electrode surface, and its hydrophobicity increased the tendency of the radical-cation intermediates to oligomerize and polymerize faster. When comparing the Q_{net} across the monomers, twice as much charge was consumed for EDOT than for MOT in both ILs. Thus, in these ILs the formation of a radical cation of the former monomer ($EDOT\cdot^+$) was probably more favored than that of the latter one ($MOT\cdot^+$). Furthermore, the Q_{net} consumed in the case of the mixed monomers, 8.20 mC in $BMIm^+BF_4^-$ and 11.84 mC in $OMIm^+Tf_2N$, were found to be close to the sum of the charges consumed separately. This showed the efficiency of polymerization was conserved during electro-co-polymerization of MOT with EDOT in both ILs.

Figure 2 (a), (b), and (c) respectively are overlays of typical post-electropolymerization CVs of PMOT, PEDOT, and PMEDOT films in fresh portions of $BMIm^+BF_4^-$, $OMIm^+Tf_2N^-$, and aq. $LiClO_4$ (0.1 M), at 50 mV/s scan rate. These CVs show that adherent homo-polymer and copolymer films were successfully electrodeposited. Figure 2 (d) displays pre-electro-polymerization background CVs and sum-CVs found by summing the CVs of PMOT and PEDOT in the respective media. It was noted that the actual CVs of the co-polymer films (Figure 2 (c)) were different from these sum-CVs. Thus, the electro-co-polymerization MOT with EDOT in the two ILs resulted in the formation of hetero-co-polymers which were intrinsically different from mere physical mixtures of the homopolymers. However, the areas under the anodic and cathodic-scan curves of the sum CVs were comparable with those of the actual CVs (Figure 2 (c)). Thus, assuming similar capacitive charging currents, the total yield of material was more or less conserved during the electro-co-polymerization – confirming the conclusion reached based on the net charges consumed.

All films exhibited multiple pairs of anodic and cathodic peaks. Conducting polymer films can exhibit multiple anodic and cathodic peaks because of several situations such as (i) being oligomeric [23] (ii) its polymer molecules segmented into short-chain repeat units [24-25] capable undergoing sequential oxidation processes, (iii) co-existence of compact and open zones respectively characterized with long chain conjugation and low degree of conjugation [11], (iv) different counter ions with different diffusion coefficients being involved during the doping and de-doping of the polymer [26-27], or (v) the reorganization of the oxidized polymer film into a thermodynamically more stable phase [28-29]. Because of the obvious complexity of the CVs under discussion, identification of the peak pairs and the associated redox reactions (couples) will not be attempted in this report. Subsequent discussions will mainly focus only on the most-prominent peaks, particularly the major anodic peaks (indicated by * in Figure 2) for which the current baselines were obvious and peak potentials easy to estimate.

3.2. Electrochemical Characterization of Films

Plots of peak-potentials ($E_{p,a}$) against the logarithm of scan rate for the major anodic peaks of the CVs of each film in the two ILs and in aq. $LiClO_4$ are shown in Figure 3 (a) and (b), respectively. Figure 4 displays the corresponding peak-height vs log of scan rate plots. Because of these peaks not being well resolved from the other (shoulder-like) anodic peaks as well as for the limited number of data points in each graph, our interpretation of the plots will only be qualitative.

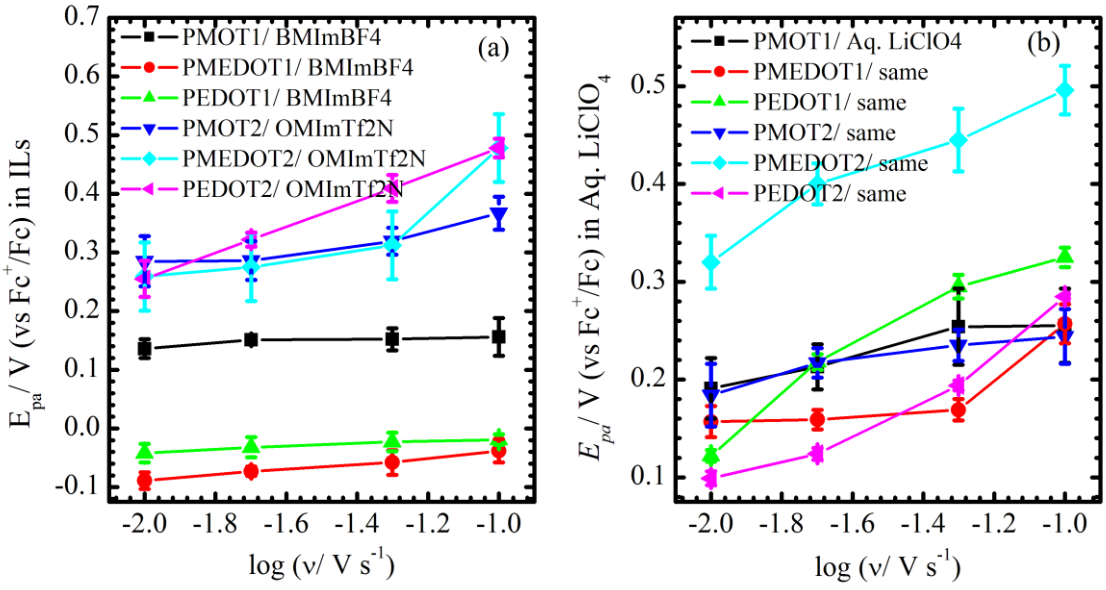

Figure 3. Peak potential vs log scan rate plots for major anodic peaks of PMOT, PEDOT, and PMEDOT films in (a) the respective ILs and (b) in aq. $LiClO_4$.

According to the results in Figure 3, qualitatively speaking, each type of film exhibited faster electrode kinetics in $BMIm^+BF_4^-$ than in $OMIm^+Tf_2N^-$, because in the case of the latter IL the $E_{p,a}$ vs log (scan rate) plots exhibited higher slopes. In aq. $LiClO_4$, both types of PMOT films (PMOT1 and PMOT2) electrochemically behaved irreversibly with similar kinetic parameters as one may judge based on the fact that the corresponding $E_{p,a}$ vs log (scan rate) plots were diagonal and of similar slopes. However, this was not true for the PEDOT and PMEDOT films: the ones prepared in $BMIm^+BF_4^-$ (PEDOT1 and PMEDOT1) exhibited faster electrode reaction than their counterparts prepared in $OMIm^+Tf_2N^-$ (PEDOT2 and PMEDOT2). Based on the CVs recorded in the respective ILs, one may note that the electro-co-polymerization of MOT with EDOT resulted in co-polymer films which were more easily oxidizable than the homo-polymers. In aq. $LiClO_4$ the co-polymer from $OMIm^+Tf_2N^-$ exhibited the most irreversible electrochemistry while that from $BMIm^+BF_4^-$ the most reversible one. The dominant tendencies of the electro-activities of these films in the three media have been differentiated as either “irreversible”, “reversible, or “quasi-reversible” in Table 1. According to Figure 4, in each case there was strong linear relationship between the respective peak height and the scan rate (ν) between 5 and 100 mV s^{-1} ($R^2 \geq 0.997$ - 0.999), indicating electrochemical systems where diffusion was not rate-limiting and that thin films were electrodeposited [22].

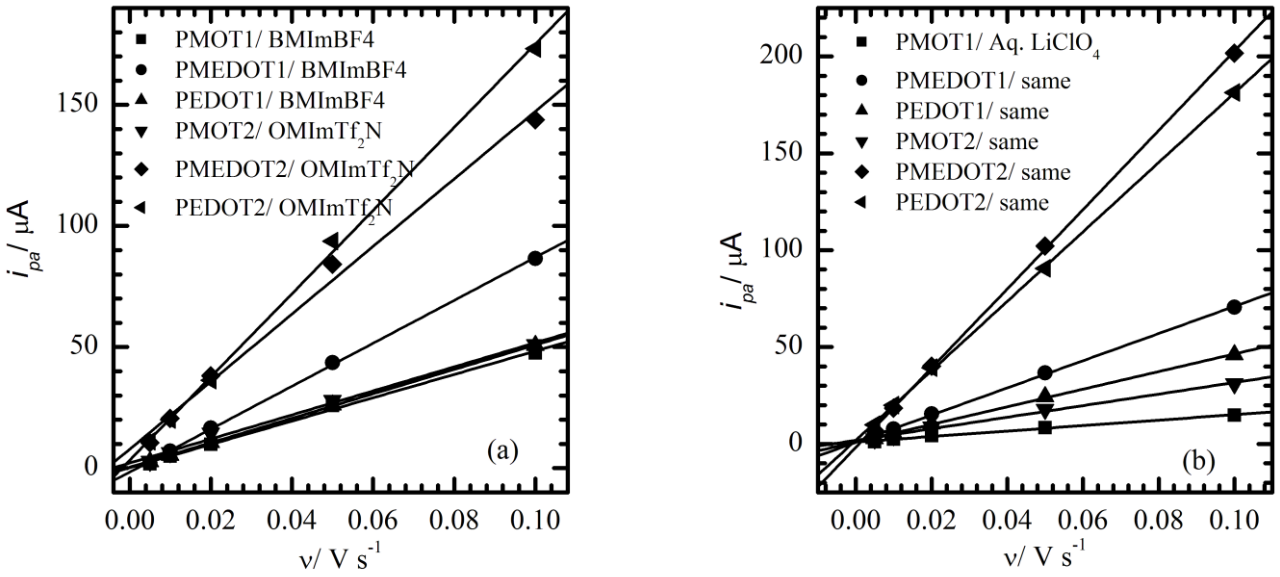

Figure 4. Dependence of the major anodic peak current of the films on scan rate in the respective ILs and in aq. $LiClO_4$. Linearity: $R^2 \geq 0.997$ - 0.999.

The effective surface concentrations (Γ/ mol cm^{-2}) in Table 1 were estimated for the electroactive polymeric segments using the equation ($i_{p,a} = \frac{n^2F^2}{4RT}\nu A\Gamma$) [30] and assuming a single-electron transfer reaction (n = 1) in each case, where A is electrode area, and F, R, and T possess their usual significances. Since the equation is strictly valid only for thin film reversible redox system, the resulting data are used here merely for comparative purposes. Considering these Γ values as being proportional to the respective polymer quantity, one may infer that similar amounts of PMOT were electrodeposited in both ILs. In contrast, significantly higher amounts of PEDOT and PMEDOT were electrodeposited in $OMIm^+Tf_2N^-$ than in $BMIm^+BF_4^-$. On transferring to aq. $LiClO_4$, all the films prepared in the former IL behaved as having higher concentration of electroactive segments than it was observed in the two ILs.

Table 1. Electrochemical reversibility and approximate surface concentrations (Γ) of the PMOT, PEDOT, and PMEDOT films as determined in different media for the first anodic peak, assuming a single electron transfer. **For irreversible cases, Γ was estimated from the i_{pa} at 10 mV s^{-1}.

	E_{pa} vs log ν	i_{pa} vs ν (N = 5, R = 0.996 – 1.000)	
Polymer/ medium	Electrochemistry	Slope/ μA s V^{-1}	Γ/ mmol cm^{-2}
PMOT1/ $BMIm^+BF_4^-$	Quasi-rev.	481±14	7.2
PMOT2/ $OMIm^+Tf_2N^-$	Quasi-rev.	497±24	7.5
PEDOT1/ $BMIm^+BF_4^-$	Quasi-rev.	504±4	7.6
PEDOT2/ $OMIm^+Tf_2N^-$	Irrev.	1718±38	**30
PMEDOT1/ $BMIm^+BF_4^-$	Irrev.	886±10	**11
PMEDOT2/ $OMIm^+Tf_2N^-$	Quasi-rev.	1395±66	21
PMOT1/ Aq. $LiClO_4$	Quasi-rev.	141±6	2.1
PMOT2/ Aq. $LiClO_4$	Quasi-rev.	298±12	4.5
PEDOT1/ Aq. $LiClO_4$	Irrev.	455±7	**8.3
PEDOT2/ Aq. $LiClO_4$	Irrev.	1791±15	**30
PMEDOT1/ Aq. $LiClO_4$	Rev.	702±10	11
PMEDOT2/ Aq. $LiClO_4$	Irrev.	2043±20	**28

3.3. UV/ Vis Absorption Spectroelectrochemical Characterization

Typical UV/Vis absorption spectra of the neutral films at E = -950 mV and after complete oxidation at E = +950 mV are shown in Figure 5 (a) to (c). The spectra exhibited peaks originating from electronic transitions from the highest occupied molecular orbitals (HOMO) to the lowest unoccupied molecular orbitals (LUMO) of conjugated thiophene repeat-units in the polymer molecules [20, 22]. The spectrum of each co-polymer film (Figure 5 (c)) was found to be very different from that would be expected (Figure 5 (d)) by summing the separate spectra of the components. Thus, the electro-co-polymerization of MOT and EDOT was successfully accomplished in both ILs. The λ_{max} of the neutral (or undoped) form of a given polymer film – hence its degree of conjugation - was the same regardless of the IL in which it had been electrodeposited. However, there were slight differences among the absorption peak-widths, which when closely inspected reveal that $OMImTf_2N$ resulted in more heterogeneous polymer films than did $BMIm^+BF_4^+$.

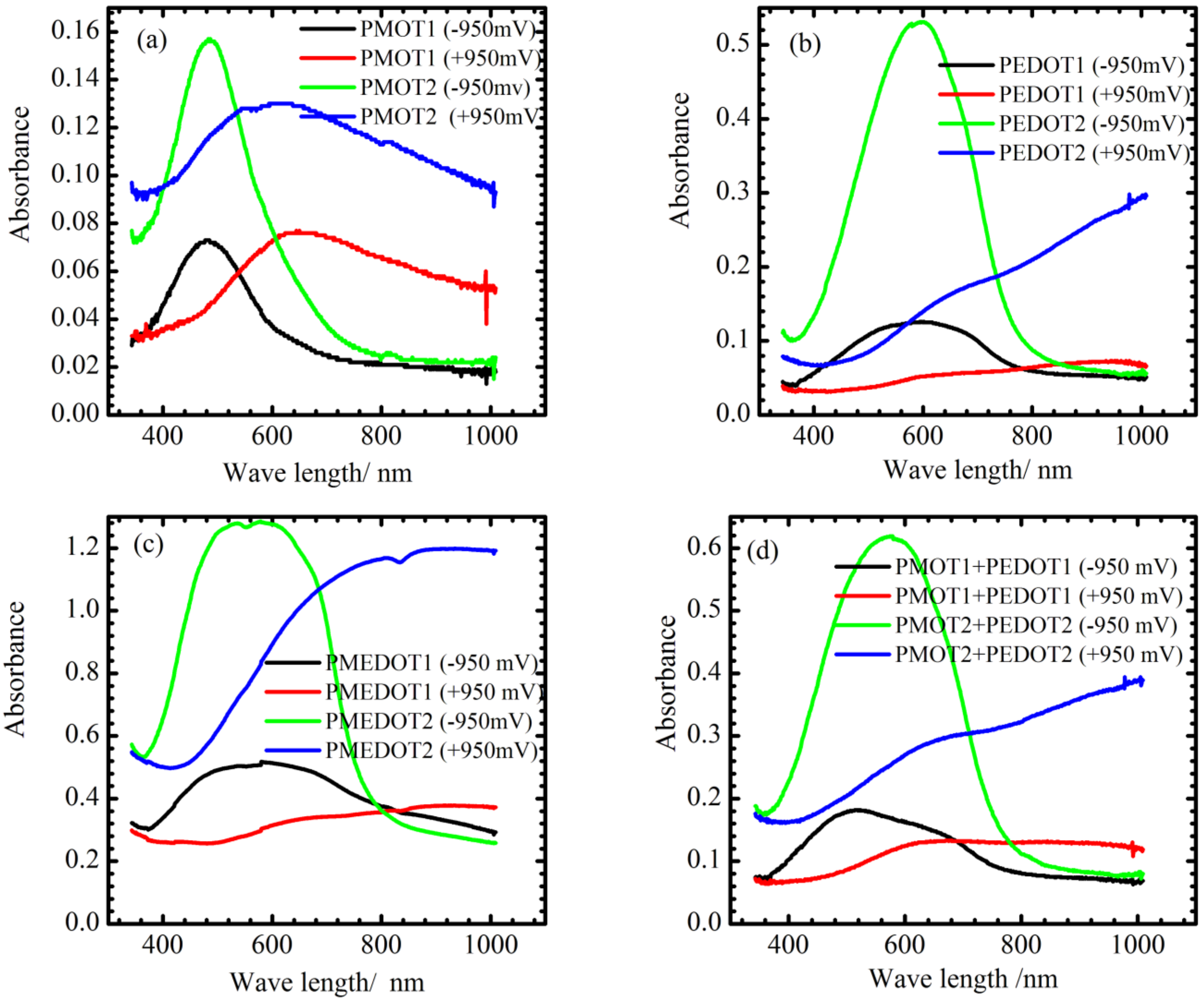

Figure 5. UV/ Vis absorption spectra recorded in aq. $LiClO_4$ (0.1 M) for completely reduced (E = -950 mV) and oxidized (E = +950 mV) films electrodeposited on ITO/ glass electrodes.

After electrochemical oxidation (or doping), a singly occupied LUMO (or SOMO) results and the absorption peaks of each films shifted to higher wavelengths, as a result of the smaller separation between the new HOMO and SOMO energy levels than that between the neutral polymer's HOMO and LUMO levels. PEDOT2 and PMEDOT2 films, respectively, exhibited larger shifts in λ_{max} than PEDOT1 and PMEDOT1 did. The reverse was observed for PMOT1 and PMOT2. Thus, the polymer molecules formed in $OMIm^+Tf_2N^-$ had higher degree of conjugation than those formed $BMIm^+BF_4^-$. The maximum absorption band was observed at about 480 nm for the neutral PMOT1 and at 485 nm for neutral PMOT2. The absorption bands of PMOT1 and PMOT2 were broad and their maximum wavelength of absorption appeared at longer wavelengths than that of a PMOT film potentiostatically polymerized in aq. $NaClO_4$/acetonitrile (λ_{max} = 400 nm) [22]. This implies the formation of a longer chain of PMOT in the ILs in the current study.

For oxidized (doped) MOT films, the corresponding 480 nm peak's intensity were attenuated and new absorption bands arose at longer wavelengths, λ_{max} 645 nm for PMOT1 and λ_{max} 600 nm for

PMOT2. It is known that the electro-oxidative doping changes the structure of PMOT's monomer units from benzenoid-type to quinoid-type [31]. The resulting oxidized-polymer has been described as a chain of radical-cationic repeat units (polarons) or diradical-cationic repeat-units (bipolarons), each being composed of five to four quinoid methoxythiophene members [19-20]. The new absorption peaks are attributed to electronic transitions from SOMO to LUMO [32-33] or HOMO to LUMO [33], respectively depending on whether the oxidized polymer is dominated by polarons or bipolarons. According to Figure 5, oxidized PMOT1 (λ_{max} 645 nm) and PMOT2 (λ_{max} 600 nm) exhibited broad absorption bands characteristic of similar energy polaronic/bipolaronic transitions of long chain oligopolythiophenes [33 34].

The λ_{max} values of PEDOT1 and PEDOT2 (both 600 nm) in the neutral-states were in agreement with that previously reported for PEDOT synthesized in 1-ethyl-3-methylimidazolium bis(triflurومethansulfonyl)imide [6]**.** The neutral forms of both PMEDOT1 and PMEDOT2 exhibited their absorption peaks around λ_{max} of 560 nm. Oxidized PMEDOT1 exhibited two broader and extensively overlapping peaks, with apparent λ_{max} values of 653 nm and 923 nm. In contrast, the oxidized PMEDOT2 exhibited an absorption plateau, which reached its height at 780 nm and extended beyond 1000 nm. The absorption bands were reversible upon electrochemical doping/ dedoping of these homopolymers and copolymer films. In the reduced state, PMOT films were red while PEDOT films were blue. After oxidation, the PMOT films underwent reversible change to blue whereas PEDOT films turned to transmissive light blue in the infrared region. PMEDOT copolymer on the other hand showed the same colour change as PEDOT. Therefore the PMOT, PEDOT and PMEDOT films produced in both ILs in this study are promising materials for applications in electrochromic devices.

3.4. Morphologies of the films

AFM images of PMOT, PEDOT, and PMEDOT films on the ITO electrodes, after oxidation in aq. $LiClO_4$, are shown in Figure 6 (a) to (f) together with that of the blank sample (Figure 6 (g)); and the corresponding root mean square roughness (R_q) values in Table 2. The morphologies of the PMEDOT films were different from PMOT's and PEDOT's. PMOT1 exhibited a more globular micro-texture and, hence, a higher porosity [6, 14-15]. Its R_q was about 129 nm. The PMOT2 film (Figure 6 (b)) was much smoother (R_q = 46.6 nm), more ordered and densely packed. PMEDOT1 was deposited as finer granules (R_q = 86.0 nm) than PMEDOT2 (R_q = 181 nm) was. The 'nano-grains" packed structures of both PEDOT1 (R_q = 9.29 nm) and PEDOT2 (R_q = 29.6 nm) are typical of three-dimensional growth mechanisms [6, 15]. The polymer molecules formed in $BMIm^+BF_4^-$ appeared to have conglomerated, resulting in a smooth and thin film with micrometric scale. Thus the nature of the IL affected the film's micro-morphology.

Table 2. Roughness values (*Rq*) of the oxidized forms of the polymer films

	PMOT1	PMOT2	PMEDOT1	PMEDOT2	PEDOT1	PEDOT2
Rq/ nm	129	46.6 nm	86.0	181	9.29	29.6

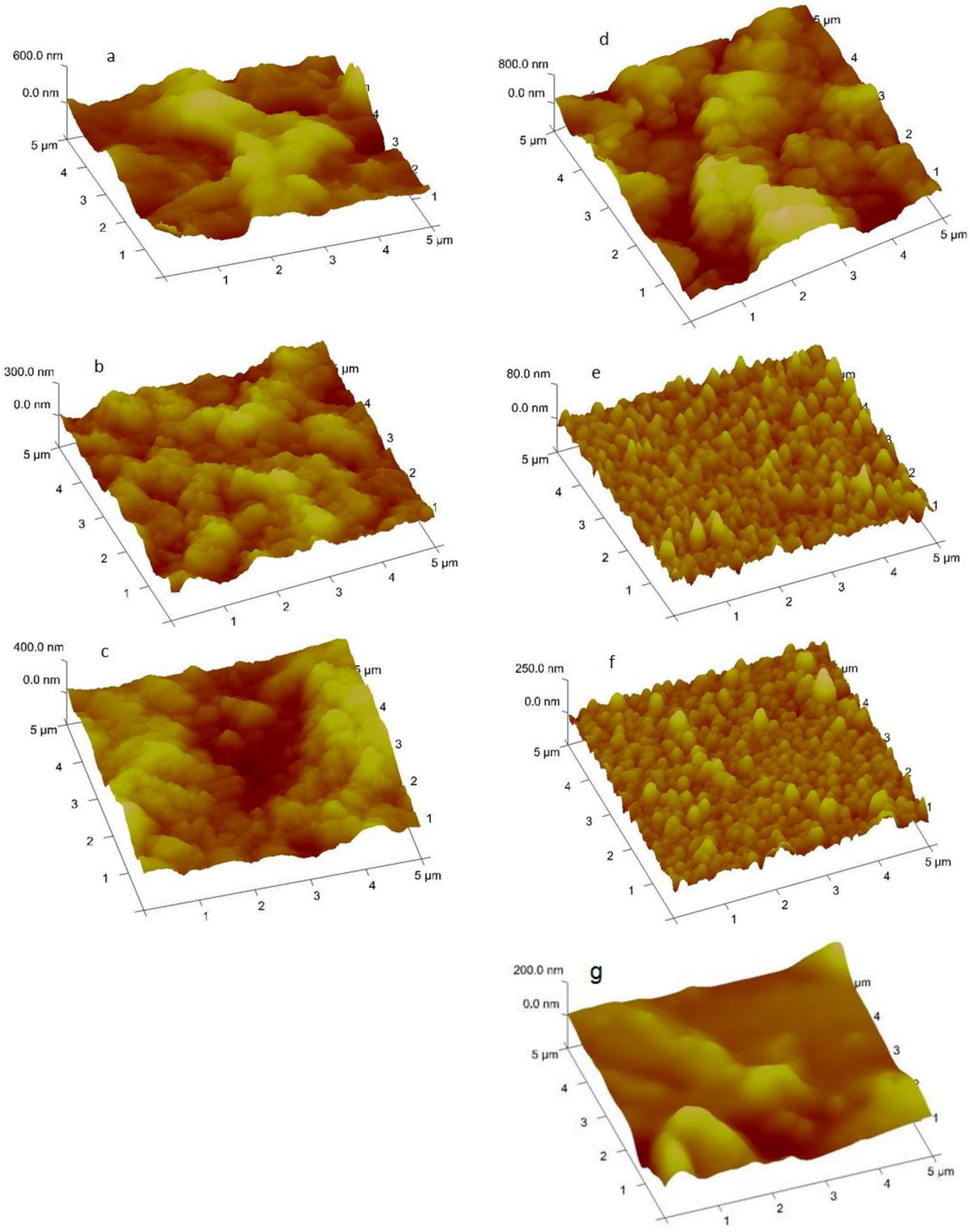

Figure 6. AFM images of oxidized (a) PMOT1, (b) PMEDOT1, (c) PEDOT1, (d) PMOT2, (e) PMEDOT2, and (f) PEDOT2 films. (g) Blank ITO electrode.

4. CONCLUSIONS

MOT was oxidized at a lower potential than EDOT in the hydrophilic IL $BMIm^+BF_4^-$, but the reverse being true in the hydrophobic IL $OMIm^+Tf_2N^-$. The MOT/EDOT mixture's oxidation-onset potentials were similar in the two ILs. According to the net-charges consumed during each electropolymerization, $OMIm^+Tf_2N^-$ enabled the deposition of thicker polymer films than did $BMIm^+BF_4^-$. Post-deposition CVs indicated the hetero-co-polymers obtained in both ILs to be intrinsically different from mere physical mixtures of the homo-polymers. The former type of films were also more easily oxidizable and exhibited at least four pairs of anodic and cathodic peaks unlike the latter ones, for which only three pairs were observed. While the amounts of PMOT electrodeposited in both ILs were similar, in contrast, significantly higher amounts of PEDOT and PMEDOT were electrodeposited in $OMIm^+Tf_2N^-$ than in $BMIm^+BF_4^-$. UV/Vis absorption spectra indicated $OMIm^+Tf_2N^-$ resulted in polymer molecules with higher degree of conjugation and more heterogeneous polymer films than did $BMIm^+BF_4^-$. According to AFM images relatively thicker and rougher films were obtained in the latter IL.

ACKNOWLEDGEMENT
The authors acknowledge financial supports from the Organization of the Prohibition of Chemical Weapons (OPCW), National Research Foundation (NRF - Republic of South Africa), and Department of Science and Technology (DST – Republic of South Africa).

References

1. E. Naudin, H.A. Ho, S. Branchaud, L. Breau, and D. Belanger, *The Journal of Physical Chemistry B,* 106 (2002) 10585-10593.
2. C. Baudequin, J. Baudoux, J. Levillain, D. Cahard, A.-C. Gaumont, and J.-C. Plaquevent, *Tetrahedron: Asymmetry,* 14 (2003) 3081-3093.
3. P. Damlin, C. Kvarnstrom, and A. Ivaska, *Journal of Electroanalytical Chemistry,* 570 (2004) 113-122.
4. P. Hapiot and C. Lagrost, *Chemical Reviews,* 108 (2008) 2238-2264.
5. O. Schneider, A. Bund, A. Ispas, N. Borissenko, S. Zein El Abedin, and F. Endres, *The Journal of Physical Chemistry B,* 109 (2005) 7159-7168.
6. K. Wagner, J.M. Pringle, S.B. Hall, M. Forsyth, D.R. MacFarlane, and D.L. Officer, *Synthetic Metals*, 153 (2005) 257-260.
7. P.S. Murray, S.F. Ralph, C.O. Too, and G.G. Wallace, *Electrochimica Acta,* 51 (2006) 2471-2476.
8. K. Sekiguchi, M. Atobe, and T. Fuchigami, *Electrochemistry Communications,* 4 (2002) 881-885.
9. E. Naudin, H.A. Ho, S. Branchaud, L. Breau, and D. Bélanger, *The Journal of Physical Chemistry B,* 106 (2002) 10585-10593.
10. W. Lu, A.G. Fadeev, B. Qi, and B.R. Mattes, *Synthetic Metals,* 135-136 (2003) 139-140.
11. H. Randriamahazaka, C. Plesse, D. Teyssié, and C. Chevrot, *Electrochemistry Communications,* 5 (2003) 613-617.
12. P. Damlin, C. Kvarnström, and A. Ivaska, *Journal of Electroanalytical Chemistry,* 570 (2004) 113-122.
13. T. Carstens, A.S.Z. El, and F. Endres, *ChemPhysChem,* 9 (2008) 439-444.
14. Y. Pang, H. Xu, X. Li, H. Ding, Y. Cheng, G. Shi, and L. Jin, *Electrochemistry Communications,* 8 (2006) 1757-1763.
15. J.M. Pringle, M. Forsyth, D.R. MacFarlane, K. Wagner, S.B. Hall, and D.L. Officer, *Polymer,* 46 (2005) 2047-2058.
16. X.C. Song, X. Wang, Y.F. Zheng, and H.Y. Yin, *Current Nanosciences,* 8 (2012) 410-413.
17. H. Tokuda, S. Tsuzuki, M.A.B.H. Susan, K. Hayamizu, and M. Watanabe, *The Journal of Physical Chemistry B*, 110 (2006) 19593-19600.
18. B.D.K. Fitchett, Travis N.; Conboy, John C., *Journal of Electrochemical Society*, 151 (2004) E219 - E225.

19. A.-C. Chang, R.L. Blankespoor, and L.L. Miller, *Journal of Electroanalytical Chemistry and Interfacial Electrochemistry*, 236 (1987) 239-252.
20. M. Fall, J.J. Aaron, N. Sakmeche, M.M. Dieng, M. Jouini, S. Aeiyach, J.C. Lacroix, and P.C. Lacaze, *Synthetic Metals*, 93 (1998) 175-179.
21. B. Dong, J. Xu, L. Zheng, and J. Hou, *Journal of Electroanalytical Chemistry*, 628 (2009) 60-66.
22. M.R.A. Alves, H.D.R. Calado, C.L. Donnici, and T. Matencio, *Synthetic Metals*, 160 (2010) 22-27.
23. Gianni Zotti and G. Schiavon, *Chemistry Materials*, 5 (1993) 620-624.
24. M. Skompska, *Electrochimica Acta*, 1998. 44: p. 357-362.
25. M. Sato, S. Tanaka, and K. Kaeriyama, *Macromolecular Chemistry and Physics*, 188 (1987) 1763-71.
26. H. Randriamahazaka, C. Plesse, D. Teyssie, and C. Chevrot, *Electrochemistry Communications*, 5 (2003) 613-617.
27. J.M. Pringle, M. Forsyth, D.R. MacFarlane, K. Wagner, S.B. Hall, and D.L. Officer, *Polymer*, 46 (2005) 2047-2058.
28. P. Marque and J. Roncali, *Journal of Physical Chemistry*, 94 (1990) 8614-17.
29. W. Domagala, M. Lapkowski, S. Guillerez, and G. Bidan, *Electrochimica Acta*, 48 (2003) 2379-2388.
30. A.J. Bard and L.R. Faulkner, *Electrochemical Methods: Fundamentals and Applications*. 1980, Wiley, pp. 718
31. A. Pron and P. Rannou, *Progress in Polymer Science*, 27 (2001) 135-190.
32. J. Cornil, D. Beljonne, and J.L. Brédas, *Journal of Chemical Physics*, 103 (1995) 842.
33. J. Cornil, D. Beljonne, and J.L. Brédas, *Journal of Chemical Physics*, 103 (1995) 834.
34. G. Louarn, M. Trznadel, J.P. Buisson, J. Laska, A. Pron, M. Lapkowski, and S. Lefrant, *The Journal of Physical Chemistry*, 100 (1996) 12532-12539.